Contrib Mineral Petrol (1983) 84:43–57

Contributions to Mineralogy and Petrology

Trace Element Geochemistry of High Alumina Basalt – Andesite – Dacite – Rhyodacite Lavas of the Main Volcanic Series of Santorini Volcano, Greece

Allan C. Mann
Department of Earth Sciences, University of Cambridge, Downing Place, Cambridge CB2 3EQ, England*

Abstract. Trace element systematics throughout the calc-alkaline high alumina basalt – basaltic andesite – andesite – dacite – rhyodacite lavas and dyke rocks of the Main Volcanic Series of Santorini volcano, Greece are consistent with the crystal fractionation of observed phenocryst phases from a parental basaltic magma as the dominant mechanism involved in generating the range of magmatic compositions. Marked inflection points in several variation trends correspond to changes in phenocryst mineralogy and divide the Main Series into two distinct crystallisation intervals – an early basalt to andesite stage characterised by calcic plagioclase + augite + olivine separation and a later andesite to rhyodacite stage generated by plagioclase + augite + hypersthene + magnetite + apatite crystallisation. Percent solidification values derived from ratios of highly incompatible trace elements agree with previous values derived from major element data using addition-subtraction diagrams and indicate that basaltic andesites represent 47–69%; andesites 70–76%; dacites ca. 80% and rhyodacite ca. 84% crystallisation of the initial basalt magma. Least squares major element mixing calculations also confirm that crystal fractionation of the least fractionated basalts could generate derivative Main Series lavas, though the details of the least squares solutions differ significantly from those derived from highly incompatible element and addition-subtraction techniques. Main Series basalts may result from partial melting of the mantle asthenosphere wedge followed by limited olivine + pyroxene + Cr-spinel crystallisation on ascent through the sub-Aegean mantle and may fractionate to more evolved compositions at pressures close to the base of the Aegean crust. Residual andesitic to rhyodacite magmas may stagnate within the upper regions of the sialic Aegean crust and form relatively high level magma chambers beneath the southern volcanic centres of Santorini. The eruption of large volumes of basic lavas and silicic pyroclastics from Santorini may have a volcanological rather than petrological explanation.

Introduction

In recent years, the genesis and evolution of the high alumina basalt – basaltic andesite – andesite – dacite – rhyodacite lavas and dyke rocks of Santorini volcano, Greece have attracted considerable attention. Nicholls (1968, 1971, 1978), on the basis of the petrography, major element chemistry and mineralogy of the major lava sequences of Santorini, collectively termed the Main Volcanic Series, proposed that the basalt – andesite – rhyodacite compositional range represented a liquid line of descent generated by the crystal fractionation of the observed phenocryst phases, calcic plagioclase + augite ± olivine ± hypersthene ± magnetite, from a parental mantle-derived basalt magma. Osborn (1976, 1979) arrived at a similar conclusion by proposing that the Main Series lavas of Santorini are analogous to the sequence of derivative liquids produced by an oxygen buffered, fractionating basaltic liquid within model experimental systems such as MgO–FeO–Fe_2O_3–SiO_2.

In contrast, several other petrogenetic models for the evolution of Santorini lavas have been proposed including 1) the partial melting of subducted ocean crust in eclogite facies mineralogy to produce either primary basaltic magmas (Puchelt 1978a) or primary andesitic magmas (Puchelt and Hoefs 1971; Pichler and Kussmaul 1972) and 2) the partial melting of sialic basement and/or contamination of basic and intermediate magmas by sialic components to produce dacite and rhyodacite magmas (Pichler and Kussmaul 1972).

The purpose of this paper is to present new trace element determinations of 20 samples of lavas and dyke rocks from the Main Series of Santorini and to show qualitatively that the observed trace element systematics are consistent with the crystal fractionation of a parental high alumina basalt magma as the dominant mechanism involved in generating the basalt – andesite – rhyodacite lava series. In addition, quantitative crystal fractionation models derived from major element compositions of both lavas and phenocryst phases using the least squares mixing program of Wright and Doherty (1970) are presented and further constrained independently by trace element considerations using the techniques of Allègre et al. (1977) involving highly incompatible trace elements.

Tectonic Setting of Santorini Volcano

The volcanic islands of the Santorini group lie within the Cyclades Islands of the S. Aegean Sea some 110 km north of Crete and constitute one of a series of late Pliocene – Recent volcanic centres which form an arcuate chain from the Gulf of Corinth to S.W. Turkey (Fig. 1). This volcanic arc and an outer predominatly sedimentary arc of Crete

* *Present address:* Department of Geology, University of London, Goldsmiths' College, Rachel MacMillan Building, Creek Road, Deptford, London SE8 3BU, England

Department of Earth Sciences Contribution No. 395

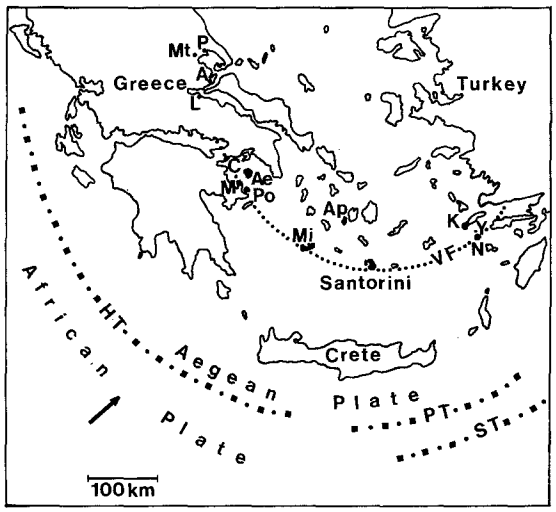

Fig. 1. Tectonic setting of Santorini volcano. Hellenic Arc volcanic centres are *C*, Crommyonia; *Ae*, Aegina; *M*, Methana; *P*, Poros; *Mi*, Milos; Santorini; *N*, Nisyros and *Y*, Yali. Other centres are *P*, Porphyrion; *Mt*, Microthebe; *A*, Achilleon; *L*, Likades Isl.; *Ap*, Antiparos and *K*, Kos (after Innocenti et al. 1981). *VF*, volcanic front. *HT*, Hellenic Trench; *PT*, Pliny Trench; *ST*, Strabo Trench. The arrow represents the regional slip vector of the Mediterranean seafloor relative to the Hellenic Arc

and the Peloponnese, collectively termed the Hellenic Arc, together with the area of the Aegean Sea behind the arc, have been interpreted as a young relatively small island arc – marginal basin system (e.g. McKenzie 1978). This island arc system has developed at a convergent plate margin as continental crust at the leading edge of the small Aegean plate moves to the S.W. overthrusting the S. Mediterranean crust of the African plate (Fig. 1). Volcanic activity along the present Hellenic Arc commenced 3.1–2.7 m.y. ago at the Pliocene – Pleistocene boundary though most activity has been Quaternary in age (Fytikas et al. 1976) and comprises the centres of Crommyonia – Aegina – Methana – Poros – Milos – Santorini – Nisyros – Yali characterised by volcanics belonging to a medium K calc-alkaline association (Keller 1982) (Fig. 1). The volcanic front corresponds to a depth of 150 km to an amphitheatral shaped Benioff zone which dips by 35–40° beneath the Aegean (Comninakis and Papazachos 1980) and Santorini volcanism has been erupted through a 25–30 km thick Palaeozoic – Mesozoic continental basement affected by both high *P/T* (Eocene) and low *P/T* (M.-U. Miocene) metamorphic episodes and associated granite intrusions (Durr et al. 1978). A postulated inner volcanic arc characterised by high K calc-alkaline volcanism (Fig. 1), has been shown to be older and/or associated with transcurrent fault and graben systems bordering the Aegean plate and hence unrelated to subduction generated volcanism along the present Hellenic Arc (Innocenti et al. 1981).

General Geology of Santorini

Of the present islands of the Santorini group, Thera, Therasia and Aspronisi are the remnants of a former stratovolcano destroyed by a paroxysmal eruption during the L. Bronze age (Pichler and Kussmaul 1980). This stratovolcano was itself a complex of several earlier volcanic centres built upon a basement of U. Triassic limestones (now forming the massif of Mt. Profitis Ilias) overthrust onto a pre-

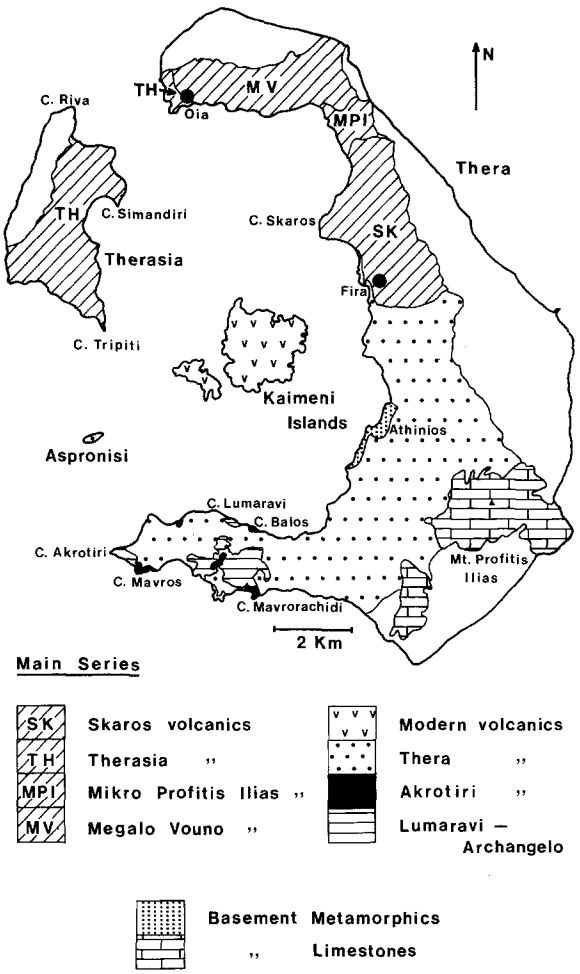

Fig. 2. Geological map of the major volcanic series and basement lithologies of Santorini (after Pichler and Kussmaul 1980)

dominantly psammitic and pelitic low grade greenschist facies metamorphic sequence of Mesozoic to Eocene age (now exposed mainly in the caldera walls) (Fig. 2). L. Pleistocene ages of 1.5–1.0 m.y. BP. have been obtained from the oldest volcanic sequence of Santorini, though most activity is younger than 100,000 years BP. and has continued through to the present day (Pichler and Kussmaul 1980). During this L. Pleistocene – Recent activity, Santorini volcanism has shown distinct differences in both the nature and composition of the volcanic products erupted from centres in the north and south of the present islands. The main volcanic activity of the southern volcanic centres was concentrated on the large and long-lived Thera volcanic complex which erupted a thick sequence of predominantly intermediate – silicic pyroclastic deposits with minor andesitic lava flows over much of the area of the present islands (Fig. 2). Two thick rhyodacite pumice and ash deposits within the Thera volcanic sequence, termed the Lower and Middle Pumice Series, have been dated approximately at 100,000 and 50,000 years BP. respectively (Pichler and Kussmaul 1980).

Contemporaneous activity from the northern volcanic centres of Megalo Vouno, the earliest products of which underly the Lower Pumice Series and hence are older than ca. 100,000 years BP., and from later volcanic centres in the Mikro Profitis Ilias, S. Therasia, Skaros and Oia/N. Therasia areas erupted a thick sequence of predominantly

basaltic to andesitic lavas and feeder dykes and volumetrically minor dacite and rhyodacite flows, domes and dykes with subordinate intercalated pyroclastics. The thick lava and pyroclastic sequences from these centres formed an overlapping complex in the north of the present islands (Fig. 2). Nicholls (1968, 1971) showed that the lavas and dyke rocks from these different centres are petrographically and chemically similar and he collectively termed the products of the northern volcanic centres of Santorini, the Main Volcanic Series.

The activity of both the northern and southern centres was terminated by the L. Bronze age Minoan eruption of Santorini, dated at $1{,}390 \pm 50$ B.C. (Hammer et al. 1980), which produced the present day caldera and blanketed all of the present day islands in a thick layer of rhyodacite pumice and ash, termed the Upper Pumice Series (Pichler and Kussmaul 1980). The subsequent eruption of viscous dacite flows and domes has led to the formation of the Kaimeni Islands within the area of the present caldera (Fig. 2).

Nomenclature and Classification of Main Series Lavas

The samples of Main Series lavas analysed in this study have been described previously by Nicholls (1968, 1971) who gives full sample locations and petrographic details. Consequently, the same nomenclature scheme has been retained in the present study. Nicholls divided the Main Series lavas on the basis of their Thornton – Tuttle Differentiation Index into basalts D.I. < 35; basaltic andesites 35–50; andesites 50–65; dacites 65–80 and rhyodacites > 80, these boundaries corresponding to significant changes in both phenocryst and groundmass mineralogy throughout the series. This scheme corresponds to more widely used discrimination schemes such as K_2O vs. SiO_2 in which the Main Series constitute a medium K volcanic series.

The Main Series of Santorini also forms a calc-alkaline series according to the alkali – lime index of Peacock (1931) and to the normative plagioclase vs. Al_2O_3 classification of Irvine and Baragar (1971). However, the moderate absolute iron enrichment shown by basaltic to andesitic lavas (Fig. 3a, b) causes the Main Series to fall within the tholeiitic field of the FeO*/MgO vs. SiO_2 classification of Miyashiro (1974).

Petrography and Mineralogy

Full details of the petrography and mineralogy of the Main Series lavas used in this study have been given by Nicholls (1968, 1971) and only a brief resumé given here. New microprobe determinations of mineral compositions in these samples have been carried out but in general they fall within the compositional ranges reported by Nicholls and are not given.

Basalts/basaltic andesites: most are massive to vesicular, porphyritic rocks, commonly with glomerophorphyritic clots of calcic plagioclase (normally zoned from $An_{93\text{-}83}$ cores to $An_{80\text{-}75}$ rims) and subordinate augite ($Ca_{45}Mg_{46}Fe_9 - Ca_{38}Mg_{46}Fe_{16}$) and olivine ($Fo_{83\text{-}72}$) phenocrysts set in an intersertal to intergranular groundmass of plagiocalse laths, granular augite, pigeonite and olivine with small magnetite octahedra and minor interstitial glass. The presence of rare hypersthene phenocrysts and magnetite microphenocrysts distinguishes basaltic andesites from petrographically similar basalts.

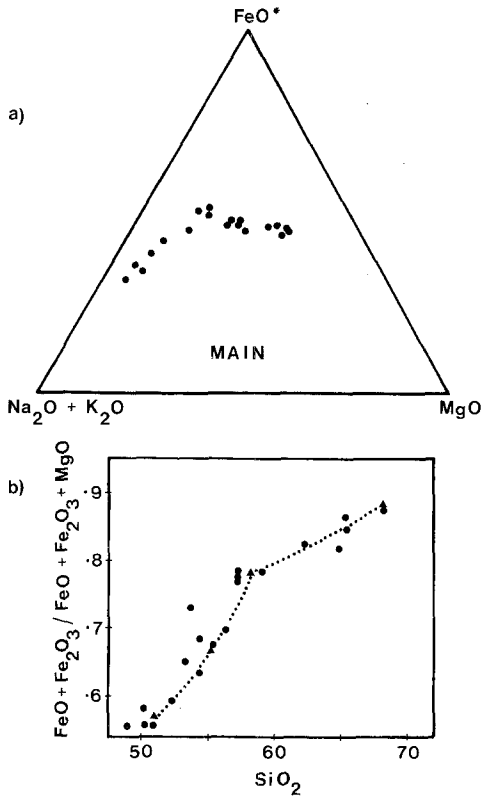

Fig. 3. **a** AFM diagram and **b** $(FeO + Fe_2O_3)/(FeO + Fe_2O_3 + MgO)$ vs. SiO_2 curve for Main Series lavas. Solid triangles are average rock analyses. All data from Nicholls (1968, 1971)

Andesites: most andesites are strongly porphyritic with abundant, generally euhedral plagioclase phenocrysts (normally zoned from An_{60} to An_{50} rims), subordinate augite ($Ca_{43}Mg_{40}Fe_{17}$) and hypersthene ($Ca_4Mg_{62}Fe_{34}$) phenocrysts with magnetite and olivine ($Fo_{62\text{-}52}$) microphenocrysts set in a flow banded pilotaxitic matrix of andesine laths, prismatic augite and pigeonite, abundant magnetite and interstitial glass. Apatite and ilmenite occur as inclusions within other phases in certain andesites.

Dacites/rhyodacite: are generally glassy, commonly flow banded rocks with isolated phenocrysts and glomeroporphyritic clots of predominantly eudhedral, weakly zoned plagioclase ($An_{50\text{-}45}$), hypersthene ($Ca_4Mg_{52}Fe_{44}$), augite ($Ca_{40}Mg_{36}Fe_{24}$), magnetite and ilmenite phenocrysts set in a glassy matrix with felted andesine prisms, acicular pyroxenes and dusty Fe – Ti oxides. Apatite occurs commonly as microphenocrysts or as inclusions within other phases.

Alteration: some Main Series lavas have undergone varying degrees of secondary and deuteric alteration, reflected petrographically by the replacement of olivine by iddingsite and rarely carbonate, the presence of quartz and zeolites as vesicle infill minerals and by the replacement of interstitial glass by fibrous aggregates of secondary alteration products. Similary, Hoefs (1978) attributed high δO^{18} values ($> +10$ per mil.) in certain Santorini lavas to low temperature hydrous alteration processes. However, the samples analysed in this study have low water contents (< 1 wt.%), appear relatively unaltered in thin section and show no significant correlations between major and trace element chemistry and any index of alteration such as

Table 1. Minor and trace element abundances in Main Series lavas, Santorini volcano, Greece

	Basalt						Basaltic andesite					
	M64	M84	M55	M89	M54	M86	M62	M87	M85	M88	M59	M180
P	248	354	355	492	559	546	536	414	428	566	671	713
	(0.05)	(0.08)	(0.08)	(0.11)	(0.12)	(0.12)	(0.12)	(0.09)	(0.09)	(0.12)	(0.15)	(0.16)
Sc	44	38	40	33	34	38	29	31	25	28	30	26
Ti	5202	5532	5102	5699	5262	5699	6961	7100	5798	6769	7505	7256
	(0.87)	(0.92)	(0.85)	(0.95)	(0.88)	(0.95)	(1.16)	(1.18)	(0.97)	(1.13)	(1.25)	(1.21)
V	295	234	261	229	221	213	281	353	200	210	187	224
Cr	76	52	67	56	60	65	34	64	49	41	51	27
Co	44	31	34	32	30	32	27	27	27	24	25	23
Ni	83	53	60	56	42	87	30	20	24	25	39	33
Rb	6	17	10	21	22	42	36	16	55	44	52	57
Sr	188	194	238	222	217	222	212	216	203	214	182	174
Y	16	23	19	25	24	26	33	26	26	32	36	42
Zr	38	78	61	90	96	134	135	79	131	142	168	193
Nb	2	3	3	4	3	4	6	4	5	4	6	7
La	4.9	8.0	6.8	9.2	8.7	15.6	10.9	7.2	14.8	14.7	15.8	16.9
Ce	12.3	18.2	16.3	22.1	18.6	29.1	28.5	17.8	33.4	34.4	37.2	37.9
Nd	7.9	11.1	9.5	12.2	11.7	16.0	14.5	9.8	16.9	17.9	19.9	22.5
Sm	2.39	3.30	2.75	3.60	3.60	3.72	4.34	2.90	4.60	4.70	5.20	5.09
Eu	0.81	1.03	0.91	1.08	1.06	1.07	1.32	1.13	1.44	1.25	1.35	1.53
Gd	3.3	4.4	3.7	3.3	3.9	4.0	4.8	3.4	5.5	5.6	6.6	6.4
Tb	0.58	0.60	0.57	0.68	0.54	0.60	0.73	0.58	1.00	0.84	1.00	0.99
Tm	0.34	0.41	0.35	0.49	0.36	0.44	0.54	0.38	0.66	0.58	0.71	0.66
Yb	1.86	2.76	2.11	2.81	2.62	2.98	3.04	2.59	4.03	3.80	4.26	4.39
Lu	0.29	0.44	0.36	0.46	0.40	0.45	0.51	0.38	0.59	0.59	0.64	0.67
Ba	113	121	114	170	148	250	201	139	210	241	220	288
Hf	2.45	2.41	2.40	2.69	2.99	3.39	4.10	2.19	4.17	4.02	4.61	5.60
Ta	0.21	0.21	0.22	0.31	0.22	0.40	0.32	0.17	0.41	0.50	0.49	0.46
Th	2.05	3.60	2.50	4.17	4.19	7.90	6.20	2.40	11.7	8.28	9.63	11.4

All values in ppm. P_2O_5 and TiO_2 also in (wt.%). P, Ti, V, Ni, Rb, Sr, Y, Zr, Nb analyses by XRF. All others by INAA. INAA analyses of samples M84, 89, 88, 59, 58, 214, 82, 294 by Dr. P. Potts (Open University). Rest by author at SURRC, East Kilbride

H_2O^+, indicating that they have been relatively unaffected by secondary alteration processes.

Major and Trace Element Chemistry

20 samples of lavas and dyke rocks from the Main Volcanic Series of Santorini, forming a compositional range from high alumina basalt through andesite to rhyodacite, have been analysed for a range of minor and trace elements and the observed concentrations are reported in Table 1. Analytical details are given in appendix I. Major element abundances in the same Main Series samples have been given previously by Nicholls (1968, 1971).

All major and trace element concentrations have been plotted on logarithmic variation diagrams using Th as a reference highly incompatible element (Figs. 4–6). Allègre et al. (1977) have shown that for a co-magmatic lava series generated solely by crystal fractionation following the Rayleigh fractionation law, such plots will approximate a straight line within each crystallisation stage of constant $\bar{D}$, with the slope of the line yielding an estimate of $\bar{D}$, the bulk distribution coefficient.

The choice of a suitable highly incompatible element throughout the whole range of the Main Series lavas is complicated by the wide range of *PTX* conditions from basalt to rhyodacite which may be expected to cause variations in $\bar{D}$ with crystallisation. However, Th behaves as a highly incompatible element throughout much of the Main Series with an observed $\bar{D}$ close to zero relative to other highly incompatible elements (i.e. Rb) and is used as a reference element in this study. Th generally shows very low distribution coefficients between plagioclase, pyroxene, olivine and liquid, behaving as a highly incompatible element in other fractional crystallisation series (Villemant et al. 1981), though Th may show relatively high magnetite/liquid distribution coefficients (0.1–1.7 within a range of Santorini magmas; Puchelt 1978b) and hence may be less incompatible within siliceous compositions involving significant magnetite crystallisation.

Major elements: Main Series lavas show extensive and regular major element variation from high alumina basalt through to rhyodacite compositions (Fig. 4). SiO_2, Na_2O and K_2O all show strong positive correlations with Th content and are progressively enriched from basalt to rhyodacite. In contrast, Al_2O_3, MgO and CaO abundances are progressively depleted throughout the series. FeO* and TiO_2 show a similar behaviour being progressively enriched from basalt to andesite before undergoing significant depletion in more siliceous compositions. This initial trend of absolute iron enrichment is reflected in an AFM diagram and in a plot of $(FeO+Fe_2O_3)/(FeO+Fe_2O_3+MgO)$ vs. SiO_2 for Main Series lavas (Fig. 3a, b). Marked inflections in the SiO_2, FeO*, TiO_2, MgO, CaO, Na_2O and $(FeO+Fe_2O_3)/(FeO+Fe_2O_3+MgO)$ vs. SiO_2 variation trends all coincide at a similar andesitic composition ($SiO_2=57$–59 wt.%; Th = 11.5–13 ppm).

Trace elements: all of the incompatible trace elements analysed (Rb, Y, Zr, Nb, REE (except Eu), Ba, Hf and

Andesite				Dacite			Rhyodacite
M58	M81	M212	M214	M261	M82	M271	M294
879	877	1007	819	794	756	846	542
(0.19)	(0.19)	(0.22)	(0.18)	(0.17)	(0.16)	(0.18)	(0.12)
25	21	24	17	15	10	19	12
7738	8607	8366	6327	4670	4457	4030	3526
(1.29)	(1.42)	(1.40)	(1.06)	(0.78)	(0.74)	(0.67)	(0.59)
198	159	171	61	46	<5	76	25
34	15	34	13	7	22	16	4
17	18	18	12	6	3	10	4
22	11	10	10	12	10	9	8
59	56	63	72	85	138	88	110
197	203	206	196	194	162	182	110
42	41	45	41	56	43	52	56
193	221	231	268	316	306	295	349
8	8	8	10	11	9	10	13
17.7	28.8	29.7	29.4	30.9	41.8	–	35.4
41.9	61.4	60.5	62.1	58.5	82.1	–	73.3
23.0	31.4	31.7	29.3	29.9	34.2	–	35.2
5.90	6.70	6.78	7.00	6.56	7.40	–	8.40
1.53	1.76	1.78	1.67	1.54	1.32	–	1.58
7.8	8.3	8.8	8.7	7.8	–	–	–
1.09	1.28	1.25	1.18	1.40	1.04	–	1.44
0.81	0.76	0.71	0.87	–	0.73	–	1.11
4.70	5.24	4.90	4.93	5.49	4.71	–	6.47
0.74	0.76	0.77	0.77	0.81	0.71	–	0.99
262	287	355	427	465	693	–	618
5.21	6.65	6.88	6.22	6.84	7.86	–	9.12
0.61	0.76	0.67	0.80	0.88	1.16	–	1.03
12.1	13.4	12.5	14.4	16.7	26.8	–	19.9

Ta) show strong positive correlations with Th content and are progressively enriched from basalt through to rhyodacite (Fig. 5). Observed enrichment factors from least fractionated basalt to rhyodacite are Rb × 10; Y × 2.9; Zr × 5.7; Nb × 4.9; La × 5.2; Yb × 3.1; Ba × 5.4; Hf × 3.8; Ta × 5.7; Th × 8.0.

In contrast, all compatible trace elements (Sc, V, Cr, Co and Ni) show strong negative correlations with Th content and are progressively depleted throughout the Main Series (Fig. 6). Marked inflections occur in all compatible element variation trends at a similar andesitic composition to those shown by most major element trends. Sr also behaves as a compatible element throughout the Main Series with near constant though slightly decreasing abundances in basaltic to dacitic lavas implying a value of $\bar{D}$ (Sr) slightly greater than 1. The Sr content of the rhyodacite (M294) is significantly lower than those of less evolved lavas. P behaves as an incompatible element in basaltic to andesitic lavas but is significantly depleted in more siliceous compositions, the inflection point again corresponding to those observed in several major and compatible element variation trends (Fig. 6).

All REE except Eu behave as incompatible elements throughout the range of Main Series lavas, with the LREE more incompatible than the M – HREE, an observation reflected in increasing La/Sm and La/Yb ratios with fractionation (Table 2). Eu behaves as an incompatible element in basaltic to andesitic lavas, though less so than all other REE, and as a compatible element in siliceous magmas (Fig. 5). Chondrite normalised REE patterns for representative Main Series lavas are given in Fig. 7 and show LREE enriched with relatively flat M – HREE patterns which are subparallel to each other, though at increasing absolute REE abundance levels from basalt through to rhyodacite compositions. Eu behaves coherently with the other trivalent REE in the least fractionated basalt samples whereas a pronounced negative Eu anomaly develops progressively in more evolved lavas, which is reflected in a plot of decreasing Eu/Eu* with increasing Th content (Fig. 7 inset).

All major and trace element variation trends show strong, regular correlations with Th content with most samples plotting close to 'best fit' regression lines. The data points suggest that most samples, though moderately to highly porphyritic, approximate compositions on a liquid line of descent from basalt through andesite to rhyodacite as proposed previously by Nicholls (1968, 1971) and Osborn (1976).

A few of the analysed samples vary systematically from the 'best fit' variation trends and may not represent liquid compositions. Basalts M64 and M86 have higher MgO, Sc, Cr, Co and Ni contents and lower incompatible element contents than comparable lavas indicating the presence of xenocrystal olivine and clinopyroxene in these samples. Basaltic andesite M87 shows anomalously high FeO*, TiO_2 and V contents and may contain or have resorbed xenocrystal magnetite. Dacite M82 has anomalously high large ion lithophile (LIL) element contents for its silica content and shows a distinctly LREE enriched pattern which crosses that of the more fractionated rhyodacite (Fig. 7). Though petrographically typical, this dacite may not be co-magmatic with the rest of the Main Series lavas or may have been modified by the operation of some secondary process

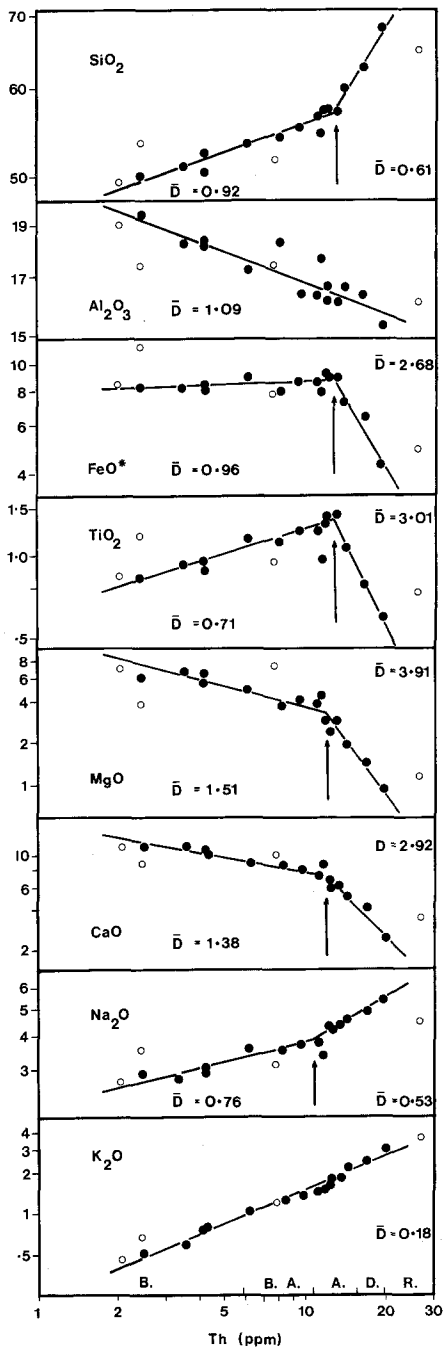

Fig. 4. Major element variation in Main Series lavas plotted on a logarithmic scale against Th content. Analyses and nomenclature from Nicholls (1968, 1971), Th this study Table 1. *B.*, basalt; *B.A.*, basaltic andesite; *A.*, andesite; *D.*, dacite; *R.*, rhyodacite. Open circles: lavas not considered to represent liquid compositions

such as crustal contamination and, together with all other samples not considered to represent liquid compositions, has been excluded from the petrogenetic modelling carried out in this paper.

The Role of Crystal Fractionation

Qualitative Evidence

Increasing incompatible element concentrations and decreasing compatible element concentrations with fractionation throughout the Main Series lavas are consistent with a model involving the crystal fractionation of the observed phenocryst phases, calcic plagioclase + augite ± olivine ± hypersthene ± magnetite ± apatite, from a parental basalt magma. In particular, the straight line variation trends within each of two distinct crystallisation stages for all elements on logarithmic variation diagrams implies that trace element systematics throughout the Main Series lavas have been governed by an exponential process. This is consistent with the closed system Rayleigh fractionation law (Allègre et al. 1977) and implies that crystal fractionation has been the dominant mechanism involved in generating the range of magma compositions within the Main Series. Similarly, the constancy of the ratios of all highly incompatible trace elements (Rb, Th, La, Zr, Nb, Ta) from basalt to rhyodacite (Table 2), reflected in straight line variation trends passing through the origin in rectilinear variation diagrams (Fig. 8), is a feature diagnostic of co-magmatic volcanic series generated by crystal fractionation processes (Treuil and Varet 1973).

Comparison between the observed chemical variation and the nature of the phenocryst phases suggests that the Main Series may be divided into two distinct crystallisation intervals each characterised by a different separating phase assemblage:

An Early Basalt to Andesite Interval. Separation of an assemblage of calcic plagioclase + augite + olivine, the dominant phenocryst phases within this stage, is consistent with the observed increase in SiO_2, FeO*, TiO_2, Na_2O, K_2O, P_2O_5 and incompatible element contents and the decrease in Al_2O_3, MgO, CaO, Sc, V, Cr, Co and Ni contents with fractionation (Figs. 4–6). The removal of this phase assemblage is also consistent with increasing absolute REE abundance levels, the greater enrichment of the more incompatible LREE and with a progressively developing negative Eu anomaly from basalt to andesite. The modal dominance of calcic plagioclase within the solid removed is indicated by the negative Eu anomaly and by the near constant Sr concentrations which, if $D_{Sr}^{plag/liq} = 1.8$–2.0 (Irving 1978), implies that plagioclase constitutes 50–60 wt.% of the solid removed. The modal proportion of olivine removed should decrease from basalt to andesite, being replaced by hypersthene in more intermediate compositions.

A later Andesite to Rhyodacite Interval. Marked inflections in the SiO_2, FeO*, TiO_2, MgO, CaO, Na_2O, P, Sc, V, Cr, Co and Ni variation trends all occur at a similar andesitic composition ($SiO_2 = 57$–59 wt.%) corresponding to some 75–80% crystallisation of the initial basalt (assuming $\bar{D}$ (Th) = O) and reflect a pronounced change in the nature of the separating phase assemblage. The petrographic appearance of magnetite as a phenocrystal or microphenocrystal phase within the Main Series corresponds to these inflections and indicates that major magnetite crystallisation causes significant depletions in FeO*, TiO_2 and V contents and to more rapidly decreasing Sc, Cr, Co and Ni contents in siliceous liquids. Inflections in the SiO_2, CaO and Na_2O trends reflect changes in the bulk distribution coefficients of these elements and partly in that of Th which may behave less incompatibly after magnetite crystallisation. Apatite precipitation, mainly as inclusions within other phases, is indicated by the marked inflection followed by decreasing P abundances in dacite and rhyodacite magmas and appears to correspond to magnetite crystallisation

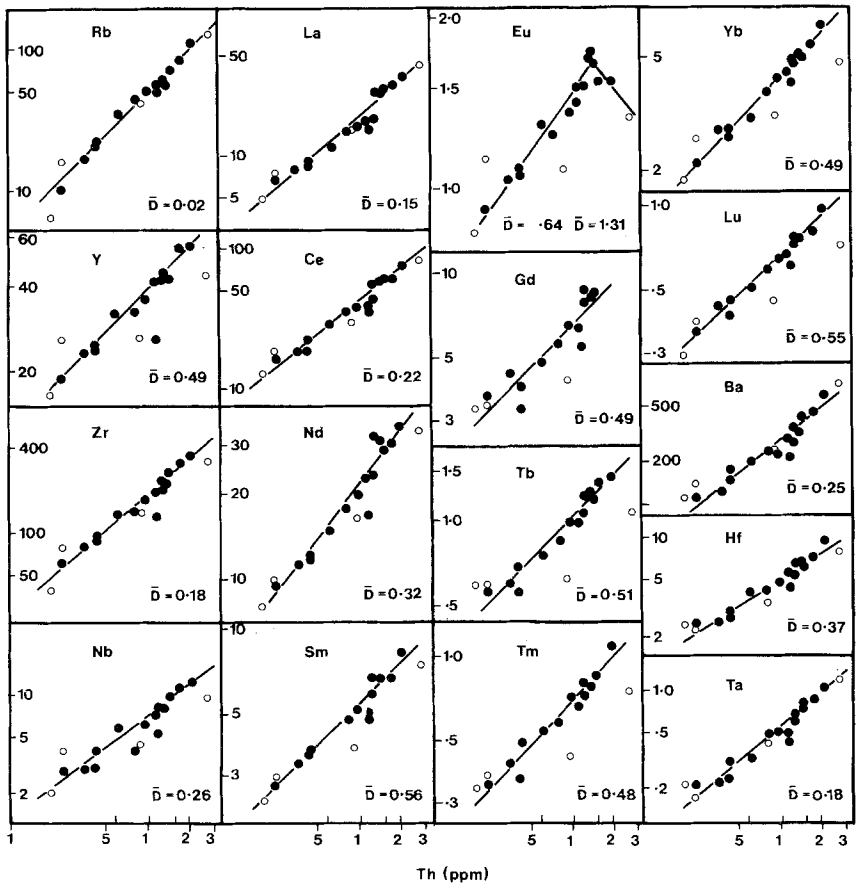

Fig. 5. Logarithmic variation diagrams of incompatible trace element concentrations vs. Th content in Main Series lavas. Symbols as in Figure 4. All data (except K – Nicholls 1968, 1971) this study Table 1. $\bar{D}$ is the observed bulk distribution coefficient derived from the slopes of the regression lines through the data points assuming $\bar{D}$ (Th) approaches zero

within the Main Series. Rapidly decreasing Sr and Eu contents in siliceous liquids suggests that plagioclase may become more modally important within the solid removed during this stage and/or that values of $D_{Sr,\,Eu}^{plag/liq}$ increase with changing *PTX* conditions during this stage. These observations suggest a separating phase assemblage again dominated by plagioclase with augite + hypersthene + magnetite + minor apatite.

Several independent geological lines of evidence also suggest that crystal fractionation of a parental basalt magma is a reasonable mechanism in generating the basaltic andesite, andesite, dacite and rhyodacite magmas of the Main Series:

i) The occurrence of caldera collapse during the Minoan and two previous paroxysmal eruptions of Santorini (Pichler and Kussmaul 1980) strongly suggests the presence of high level, sub-volcanic magma chambers in which crystal fractionation processes may operate during periods of quiescence of the volcano.

ii) The presence of cognate gabbroic xenoliths within some Main Series lavas and more commonly within other Santorini volcanic series (e.g. the Modern Series; Nicholls 1968, 1971), which show cumulate textures and a mineralogy of calcic plagioclase, augite, olivine, hypersthene and magnetite compositionally similar to the observed phenocryst phases within the lava series, also provides strong evidence for the operation of crystal fractionation processes within Santorini magma systems.

iii) Nicholls (1978) showed that high alumina basalt of $SiO_2 = 51$–52 wt.% is the most frequently reported composition within 76 literature analyses of pre-caldera Santorini lavas and field observations indicate that basic lavas and dyke rocks predominate within the northern volcanic centres with progressively smaller proportions of more evolved compositions (Nicholls 1968, 1971). Although this does not objectively reflect the true volume relations of Santorini magmas, it is consistent with a proposed crystal fractionation model though the large volumes of silicic magma erupted from the southern centres distorts the apparently straightforward volume relations shown by the Main Series lavas.

iv) Osborn (1976, 1979) and Nicholls (1968, 1971) have interpreted the curve of $(FeO + Fe_2O_3)/(FeO + Fe_2O_3 + MgO)$ vs. SiO_2 for the Main Series lavas (Fig. 3b) as being analogous to the course followed by a fractionating model basaltic liquid in experimental systems under conditions of moderate and near constant oxygen fugacity levels. An early subvertical trend of moderate absolute iron enrichment corresponds to silicate crystallisation from the oxygen buffered basalt magma continuing until the liquid reaches the silicate – magnetite boundary curve with further fractionation resulting in strong silica enrichment with little or no iron enrichment in residual liquids. The correspondence of the appearance of major phenocrystal magnetite and marked inflections in many major, trace element and the $(FeO + Fe_2O_3)/(FeO + Fe_2O_3 + MgO)$ vs. SiO_2 variation trends at a similar andesitic composition supports this interpretation. Nicholls (1968, 1971) showed from $f_{O_2} - T$ estimates derived from coexisting Fe–Ti oxides that Main Series lavas do define an $f_{O_2} - T$ curve close to the QFM buffer, though more recent experimental work on basaltic andesite M85 suggests higher magmatic f_{O_2} levels above the NNO buffer (Osborn and Rawson 1980).

v) Few Sr^{87}/Sr^{86} isotope ratios of Main Series lavas

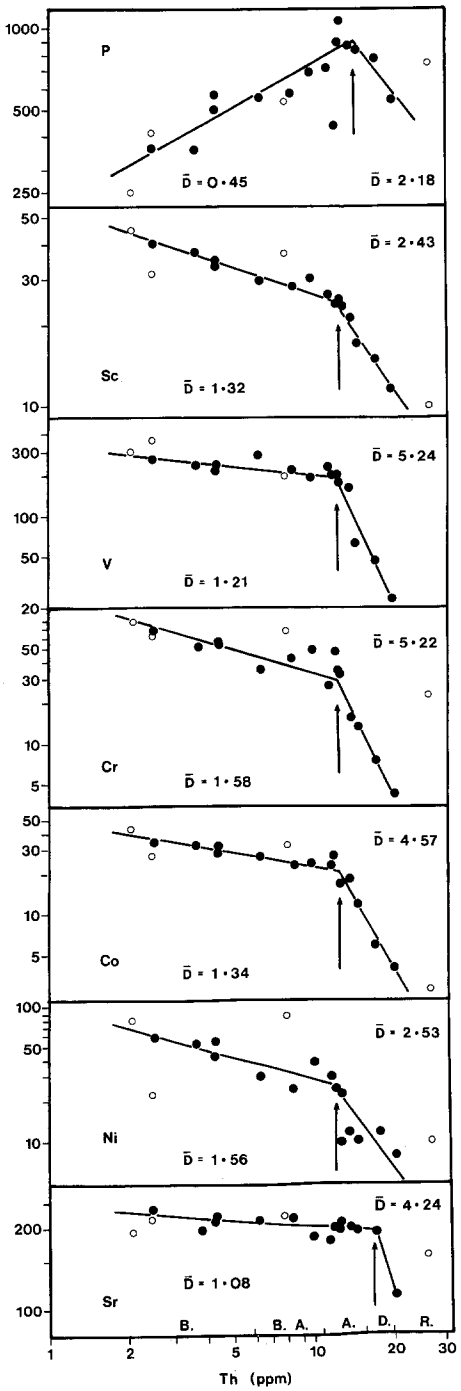

Fig. 6. Logarithmic variation diagrams of compatible element concentrations vs. Th content in Main Series lavas. All data this study Table 1. Symbols as in Figs. 4, 5

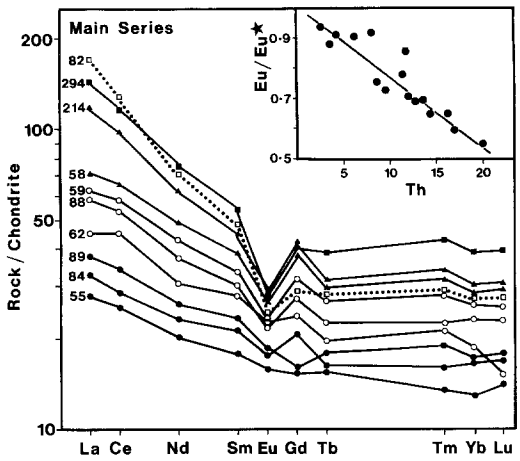

Fig. 7. Chondrite normalised REE patterns for representative Main Series lavas. Normalised to chondrite values from Evensen et al. (1978). Solid circles – basalts; open circles – basaltic andesites; solid triangles – andesites; solid squares – rhyodacite and open squares – dacite M82. Inset: the progressive development of a negative Eu anomaly as Eu/Eu* vs. Th content in Main Series lavas

Table 2. Trace element ratios in Main Series lavas

	Basalt	Basaltic Andesite	Andesite	Dacite – Rhyodacite
K/Rb	432–294	217–251	219–274	224–248
K/Ba	42–37	43–59	44–54	41–45
K/La	623–744	720–841	531–732	683–720
La/Sm	2.4–2.6	2.5–3.3	3.0–4.4	4.2–4.7
La/Yb	2.9–3.3	3.6–3.9	3.8–6.1	5.5–5.6
La/Nb	2.3–2.9	1.8–3.7	2.2–3.7	2.7–2.8
La/Ta	30–40	29–37	29–44	34–35
K/Zr	65–71	64–95	67–71	67–73
Ba/Zr	1.5–1.9	1.3–1.7	1.3–1.6	1.5–1.8
Zr/Hf	25–33	31–35	33–43	38–46
Zr/Nb	20–32	23–36	24–29	27–29
Nb/Ta	13–14	8–19	11–13	13

Data this study Table 1

are yet available in the literature. A value of 0.7056 has been reported for a Skaros andesite (Pichler and Kussmaul 1972) whereas Pe and Gledhill (1975) report values of 0.7049 ± 0.0008 for basalt M89 and 0.7056 ± 0.0002 for rhyodacite M294 of Nicholls (1968, 1971) and the present study. New unpublished Sr^{87}/Sr^{86} ratios for Santorini lavas show a range from 0.7047–0.7051 (M. Barton pers. comm.) and show no correlation with chemical variation. The relative constancy of Sr^{87}/Sr^{86} ratios throughout the magma series is consistent with crystal fractionation though the range of reported values may indicate the operation of additional processes such as crustal contamination or secondary alteration.

Quantitative Models

Major Elements. In order to test the proposed crystal fractionation model for the Main Series, least squares mixing calculations have been carried out using the whole rock major element analyses reported by Nicholls (1968, 1971), major element compositions of phenocryst phases determined by microprobe and the least squares petrological mixing program of Wright and Doherty (1970). Basalt M84 was chosen as the parent composition due to its near aphyric texture and calculations carried out stepwise to generate successive basaltic and basaltic andesite liquids. A basaltic andesite was then assumed parental to andesitic liquids which were in turn assumed parental to more fractionated dacites and rhyodacite. Calculations over shorter intervals produced considerable loss of precision whilst over longer intervals unacceptably high values of Σr^2 were found. Plagioclase and olivine were input as end-member compositions with the program calculating the An and Fo

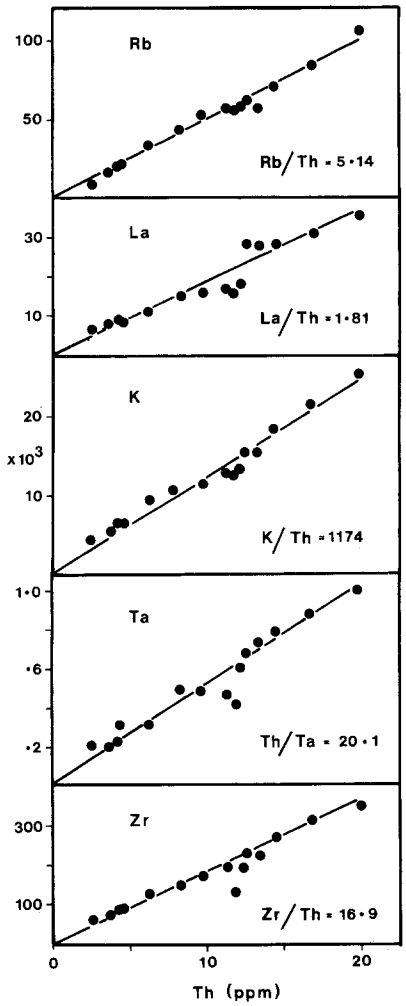

Fig. 8. Rectilinear variation diagrams of highly incompatible trace element concentrations (Rb, La, K, Ta and Zr) vs. Th content in Main Series lavas

content of the phases removed (Table 3). Augite, hypersthene and magnetite were input as compositions appropriate to their position within each crystallisation stage.

The results of the least squares calculations are given in Table 3 and indicate that basaltic andesites may be generated by up to 50% crystallisation of the parental basalt on the removal of a solid assemblage dominated by calcic plagioclase (48–55 wt.%) with augite (25–30 wt.%) and olivine (15–21 wt.%). Andesites may be generated by up to 40% crystallisation of an intermediary basaltic andesite and by up to 60% crystallisation of the parental basalt. The solid removed is again dominated by calcic plagioclase (52–55 wt.%) and augite (34–38 wt.%) though the proportion of olivine removed (16–10 wt.%) decreases with fractionation. Minor magnetite joins the separating phase assemblage between andesites M212–214 (ca. 5 wt.%). Main Series dacites and Skaros rhyodacite may be generated by up to 35% crystallisation of an andesitic magma and by up to 75% crystallisation of the assumed parent basalt. The weight fraction of plagioclase in the solid removed increases to a maximum of 64 wt.% whereas that of augite decreases from 23 – 10 wt.%. Hypersthene becomes an important phase (ca. 18 wt.%) along with magnetite (6–12 wt.%) and minor apatite (< 1 wt.%) in the solid removed during this stage.

Discrepancies between the observed and calculated compositions of the derivative daughter magmas, as represented by the sum of the squares of the residuals Σr^2, generally have low values less than or close to 1, though several are in the range of 1–2 (Table 3). Although it is not possible to apply rigorous statistical criteria to the acceptability of such least squares solutions (Banks 1979), previous workers have assumed arbitrary upper limits of $\Sigma r^2 = 1.5$ (e.g. Luhr and Carmichael 1980). According to this criterion, the least squares calculations for the Main Series lavas represent a reasonable fit between the observed and calculated derivative magmas and indicate that the proposed crystal model is reasonable.

Table 3. Results of crystal fractionation modelling

	Basalt M84→							Basaltic Andesite M85→				Andesite M214→	
	→89	→54	→62	→85	→88	→59	→180	→58	→81	→212	→214	→261	→294
Plagioclase	3.9%	7.7%	17.8%	19.0%	18.3%	25.7%	26.2%	12.0%	13.7%	14.3%	20.1%	6.3%	22.2%
Clinopyroxene	2.2%	–	9.7%	10.2%	11.4%	11.5%	11.7%	8.9%	9.0%	8.8%	14.1%	3.4%	3.4%
Olivine	–	4.3%	4.9%	7.4%	8.0%	8.8%	9.2%	2.3%	1.9%	2.6%	2.3%	–	–
Orthopyroxene	–	–	–	–	–	–	–	–	–	–	–	2.7%	5.8%
Ti-magnetite	–	–	–	–	–	–	–	–	–	–	1.9%	1.8%	2.1%
Apatite	–	–	–	–	–	–	–	–	–	–	–	0.1%	0.1%
Σr^2	0.61	2.06	0.37	1.44	1.02	1.08	1.60	0.53	0.23	0.16	0.09	0.36	0.71
F (Least Squares)	93.9%	88.0%	67.6%	63.4%	62.3%	54.0%	52.9%	48.7%	47.8%	47.1%	39.1%	33.5%	25.9%
F (Incompatible)	83.6%	81.6%	52.6%	30.8%	41.1%	35.0%	30.7%	29.3%	28.6%	27.9%	24.3%	20.8%	16.8%
F (Addition-Subtraction)				(46%)						(33%)		(18%)	(15%)
An calculated	100	100	100	100	100	97	100	100	100	100	83	60	50
(observed)	93–87	93–83	90–81	–	90–83	90–87	86–80	84–87	80–70	80–50	75–50	55–40	55–40
Fo calculated	100	100	100	70	62	54	59	62	70	70	70	–	–
(observed)	82–77	77–72	79–71	–	76–71	78–71	73–69	70–53	70–53	70–53	70–53	–	–

Major element analyses and values of F (additon – subtraction) from Nicholls (1968, 1971). Σr^2 – sum of squares of residuals between observed and calculated compositions. F – weight fraction of residual liquid. F (incompatible) – averge of the ratio C_o/C_L for Rb and Th abundances where C_o is the concentration in basalt M84

Trace Elements. Assuming Rayleigh fractionation, the concentration ratio of all highly incompatible trace elements (i.e. $\bar{D}$ approaching zero) in the initial liquid to that in derivative liquids should approximate values of F, the weight fraction of residual liquid (i.e. $C_O^*/C_L^* \approx F$ as $\bar{D} \approx O$; Allègre et al. 1977). Both Rb and Th behave as highly incompatible elements throughout most of the Main Series (Fig. 5) and have concentration ratios (using M84 as the parent basalt) yielding approximations of F which are compared with those derived from least squares calculations in Table 3.

The values of F (incompatible) indicate that basaltic andesites represent 47–69%; andesites 70–76%; dacites ca. 80% and rhyodacite ca. 84% crystallisation (i.e. 100–F%) of the assumed parent basalt. However, it is also apparent that the values of crystallisation derived from incompatible element ratios are higher, on average up to 20% greater, than those indicated by the least squares calculations (Table 3). Similar discrepancies between percent solidification values derived by major and incompatible element approaches have been observed in other volcanic series (e.g. Gill 1978, 1981) and may result from several factors including a) the assumed crystal fractionation model may be incorrect or incomplete, b) the major element least squares solutions may be incorrect, c) crystal fractionation may operate under open system conditions and hence deviate from Rayleigh fractionation behaviour (O'Hara and Mathews 1981).

On the basis of addition – subtraction diagrams using the same major element data, Nicholls (1968, 1971) proposed that an average Main Series basaltic andesite may represent 54%, average andesite 67% and average dacite 82% crystallisation of an initial basalt magma. The closer correspondence of the percent solidification values from the addition – subtraction calculations with those indicated by incompatible element ratios (Table 3) suggests that in this case, the solutions to the least squares calculations are incorrect, indicating percent solidification values up to 20% lower than they should be. There is no 'a priori' reason to suppose that least squares solutions to mixing problems are necessarily more correct than the wide range of possible solutions which may fit the data within acceptable confidence limits and though they indicate if the proposed model is reasonable, they do not specify how reasonable. This example illustrates the possible errors inherent in the acceptance of unconstrained least squares mixing solutions and suggests that in some cases, the decoupling of major and trace elements, as indicated by discrepancies between least squares and incompatible element considerations, may be more apparent than real.

Estimation of Bulk and Individual Distribution Coefficients. Estimates of $\bar{D}$ for all major and trace elements can be derived from the slopes of the variation trends in Figs. 4–6, assuming $\bar{D}$ (Th) approaches zero. Within the Main Series, only Rb behaves as a highly incompatible element with $\bar{D}$ (Rb) = 0.02 whereas La (0.15); K, Zr, Ta (0.18); Ce (0.22); Ba (0.25); Nb (0.26); Nd (0.32) and Hf (0.37) show decreasing incompatible behaviour in that order with the M – HREE and Y (0.48–0.56) less incompatible reflecting their preferential removal by clinopyroxene ($D_Y^{cpx/liq} = 0.5$–4.0: basic – acid; Pearce and Norry 1979). The less incompatible behaviour of Hf relative to Zr, reflected in a slight increase in the Zr/Hf ratio with fractionation (Table 2), may also reflect clinopyroxene crystallisation (e.g. $D_{Zr}^{cpx/liq} = 0.27 \pm 0.15$; $D_{Hf}^{cpx/liq} = 0.48 \pm 0.12$; Villemant et al. 1981).

Cr, Ni, MgO, Co, Sc and V show decreasing compatible behaviour in basaltic to andesitic compositions reflecting significant olivine and clinopyroxene precipitation (Figs. 4, 6). The greater compatibility of CaO, Sr and Eu in siliceous liquids reflects an increased weight fraction of plagioclase in the solid removed (ca. 0.50–0.65; Table 3) and an increase in the values of $D_{Sr}^{plag/liq}$ with increasing silica content and decreasing temperature of the melt (Drake and Weill 1975). Major magnetite crystallisation in andesitic liquids is marked by the compatibility of FeO* and TiO_2 (Fig. 4), by the greater compatibility of MgO, Sc, V, Cr, Co and Ni and by the greater incompatibility of SiO_2 in andesitic to rhyodacite magmas. Apatite precipitation is marked by the compatible behaviour of P ($\bar{D} = 2.18$) within the same crystallisation interval (Fig. 6).

The observed bulk partition coefficients within each crystallisation stage of the Main Series can yield estimates of averaged individual mineral/liquid distribution coefficients if the weight fractions of the precipitating phases are known (and vice versa). This has been carried out for the Main Series lavas using values of mineral weight fractions in the solid removed provided by the least squares mixing solutions (Table 3). Although the least squares solutions are suspect, the weight fractions of separating phases are of a similar order to those obtained by Nicholls (1968, 1971) using addition – subtraction diagrams and make a useful first approximation. Other simplifying assumptions have been made 1) literature values of certain mineral/liquid distribution coefficients have been assumed in order to deduce more critical values 2) in order to estimate magnetite/liquid coefficients, the values of other phases in this stage have been assumed from the literature (orthopyroxene) or have been assumed to be identical to those obtained in the previous basalt – andesite crystallisation stage. The estimated mineral/liquid distribution coefficients for the Main Series are given in Table 4 and may be compared with the range of natural values from a range of Santorini magma compositions reported by Puchelt (1978b) and with a compilation of literature values for andesitic liquids presented by Gill (1981 Table 6.3).

In general, the empirically derived mineral/liquid distribution coefficients are of a comparable order to and fall within the range of natural values observed in Santorini volcanics and to the average values for andesitic liquids (Table 4). However, the estimated value of $D_{Ti}^{cpx/liq}$ is significantly higher than expected from the TiO_2 contents of coexisting clinopyroxenes (0.40–0.75 wt.%) and groundmass (0.90–1.45) in Main Series lavas and may suggest that minor magnetite may precipitate and be removed, possibly as inclusions within other silicate phases, prior to major magnetite crystallisation within andesitic liquids. Values of $D_{Nb,\,Hf,\,Ta}^{cpx/liq}$ are also significantly higher than expected from previous literature values and may also reflect minor magnetite separation within the basalt – andesite stage given that Puchelt (1978b) reported values of $D_{Hf}^{magn/liq} = 0.5$–20.3 and $D_{Ta}^{magn/liq} = 0.4$–3.7 in Santorini magmas (Table 4). Similarly, the observed bulk distribution coefficient of P within the basalt to andesite stage ($\bar{D}$ (P) = 0.45; Fig. 6) is too high to be accounted for by plagioclase + augite + olivine separation given the expected mineral/liquid distribution coefficients for these phases and may indicate early separation of apatite prior to the main apatite crystallisation in

Table 4. Estimated mineral/liquid distribution coefficients for Main Series lavas

	Plagioclase/ Liquid	Clinopyroxene/ Liquid	Olivine/ Liquid	Magnetite/ Liquid	Orthopyroxene/ Liquid
Sc	(0.03)	4.20 2.5–17[a] 1.8–18[b]	(0.30)	13.3 1–3[a] 2–14[b]	(3.0)
Ti	(0.05)	2.22	(0.05)	26	(0.5)
V	(0.10)	3.83 0.9–18[a]	(0.05)	44 24–63[a]	(1.5)
Cr	(0.05)	4.68 10–245[a] 4.7–87[b]	(1.00)	40 1–166[a] 36[b]	(3.0)
Co	(0.05)	(1.5)	5.82 5.7–6.2[b]	41 4–25[a] 19–98[b]	(1.5)
Ni	(0.05)	(2.0)	6.22	19 4–19[a]	(2.0)
Rb	0.04 0.02–0.19[a] 0.04–0.05[b]	–	–	–	–
Sr	1.91 1.3–3.2[a]	(0.10)	(0.01)	–	–
Y	(0.04)	1.56 0.09–1.5[a] (Yb) 0.40–2.6[b] (Yb)	(0.02)	–	–
Zr	(0.05)	0.48 0.18–0.34[a]	(0.03)	–	–
Nb	(0.05)	0.79 0.30[a]	(0.03)	–	–
La	(0.20)	0.12 0.1–0.4[b]	(0.03)	–	–
Sm	(0.15)	1.57 0.09–1.4[a] 0.20–1.3[b]	(0.03)	–	–
Eu	0.62 0.06–1.3[a] 0.08–2.0[b]	(1.50)	(0.03)	–	–
Yb	(0.05)	1.56 0.09–1.5[a] 0.40–2.6[b]	(0.03)	–	–
Lu	(0.05)	1.72 0.09–1.5[a] 0.60–2.8[b]	(0.03)	–	–
Ba	0.42 0.05–0.36[a]	(0.05)	(0.03)	–	–
Hf	(0.05)	1.13 0.18–0.34[a] 0.40–2.8[b]	(0.03)	–	–
Ta	(0.05)	0.49 0.30[a]	(0.03)	–	–

Values in brackets are assumed from literature. Observed values of $\bar{D}$ employed are from Figures 5 and 6. Mineral weight fractions from least squares calculations are 1. Basalt to Andesite: Plag: Cpx: Oliv = 0.55:0.30:0.15 and 2. Andesite to Rhyodacite: Plag: Cpx: Opx: Magn = 0.59:0.15:0.15:0.10

[a] Distribution coefficients for andesitic liquids (Gill 1981 Table 6.3)

[b] Distribution coefficients for a range of Santorini magmas (Puchelt 1978b)

andesitic liquids. Local concentrations of P in the liquid may cause local crystallisation of apatite as minute crystals which may be included in rapidly growing phenocrysts, preventing the enrichment of P in the liquid expected on the separation of P_2O_5 poor phases (Green and Watson 1982).

The estimated mineral/liquid distribution coefficients are of poor precision given the assumptions made in their derivation and cannot be used to prove that Main Series lavas are related by crystal fractionation in that they have been derived in a circular fashion by assuming that crystal fractionation has been the dominant mechanism in their generation. Nevertheless, the comparable order of the estimated mineral/liquid distribution coefficients to natural values observed in a range of Santorini magma compositions provides supporting evidence that the proposed crystal fractionation model is reasonable.

Open or Closed System Crystal Fractionation? Main Series lavas do not show the chemical features expected of lavas generated in open system magma chambers undergoing periodic replenishment, periodic tapping and continuous fractionation as modelled by O'Hara and Mathews (1981). However, several of the rhyodacite plinian pumice fall deposits of Santorini, most notably the Minoan fall deposit, contain xenoliths of quenched basaltic andesite pumice (Sparks et al. 1977) indicating at least some open system behaviour within Santorini magma systems. In addition, Osborn and co-workers have proposed that the calc-alkaline volcanic series in general (e.g. Osborn 1979; Eggler and Osborn 1982) and the Main Series of Santorini in particular (Osborn 1976) represent a series of derivative liquids produced by the crystal fractionation of a basaltic liquid under open system, oxygen buffered conditions. The observation that major and trace element variation within Main Series lavas approaches and can be successfully accounted for by closed system Rayleigh fractionation may reflect the particular conditions prevailing during evolution of the Main Series but more generally may reflect the inability of the highly incompatible element techniques used in this study to discriminate, at the present level of sampling and analytical precision, between the open system (calc-alkaline) and closed system (tholeiitic) crystal fractionation trends of Osborn (1979).

The Role of Other Mechanisms in Generating Main Series Lavas

Straight line variation trends and marked inflection points on logarithmic variation diagrams and the absence of petrographic evidence of disequilibrium which can be unambiguously attributed to magma mixing (i.e. incompatible phase assemblages) precludes the simple binary mixing of basic and silicic magmas in generating the range of Main Series lavas, though individual lavas may be the product of mixing two magmas themselves mutually related by crystal fractionation on the liquid line of descent. Similarly, the relatively high Sc, Y and Yb contents and the absence of strongly fractionated REE patterns (reflected in low La/Yb ratios of 2.8–6.0; Table 2) in Main Series lavas precludes a significant role for garnet as a fractionating or residual phase in their generation and indicates that even the least fractionated basalts were not in equilibrium with a garnet bearing souce prior to eruption. Amphibole is not an observed phenocryst or groundmass phase within Main Series

lavas and they do not show the chemical features expected from significant amphibole participation in their generation, i.e. near constant or decreasing Y contents ($D_Y^{amph/liq.}$ = 1.0–6.0: basic-acid; Pearce and Norry 1979) and M-HREE contents, generating V-shaped REE patterns with minima at Dy–Ho (Nicholls and Harris 1980).

In general, the relatively constant Sr^{87}/Sr^{86} ratios (M. Barton pers. comm.) and the straight line major and trace element variation trends (Figs. 4–6) provide no evidence for significant sialic contamination within the observed basalt to rhyodacite lavas. Similarly, the observation that all andesite, dacite and rhyodacite lavas have ratios for highly incompatible trace elements (e.g. K/La, Nb/Ta etc. Table 2) identical to those of mantle derived basalts suggests a common source for all Main Series lavas and rules out the partial melting of unrelated sialic basement in generating Main Series intermediate-silicic magmas. However, only a few silicic samples have been analysed in this study and more complex models involving melting of or contamination by earlier volcanic or plutonic basement cannot be discounted. In addition, the extent to which the parental basalt magma may have been modified by interaction with the thick sialic crust of the Aegean plate cannot be ascertained on the present evidence and requires further chemical and isotopic studies.

Regional and Global Comparisons

The Main Series lavas of Santorini have broadly comparable major element compositions to the basalt – andesite – dacite – rhyolite lavas of the other volcanic centres of the Hellenic Arc, though basalts are rare in these centres which are dominated by andesite and dacite (Crommyonia, Aegina, Methana, Poros, Christiana Islands, Nisyros) and by rhyolite (Milos, Yali) (Keller 1982). Hellenic Arc lavas show typical calc-alkaline characteristics with AFM trends of moderate to no iron enrichment and medium K contents with K_2O at 60 wt.% SiO_2 of 1.2–2.0, typical of many orogenic calc-alkaline series (Keller 1982). Few systematic trace element studies of Hellenic Arc lavas are yet available though Innocenti et al. (1981) report major and trace element data on 17 lavas from Crommyonia, Aegina, Methana, Milos and Nisyros. In general, the basaltic andesite – rhyolite lavas of these centres have comparable trace element systematics to Main Series lavas (Fig. 9), interpreted as evidence for the operation of low pressure plagioclase + clinopyroxene + olivine + magnetite + orthopyroxene + apatite crystal fractionation in the generation of the lava series of the other Hellenic Arc centres (Innocenti et al. 1981). Reported Sr isotope ratios show considerable ranges for individual centres e.g. Santorini 0.7040–0.7060; Nisyros 0.7037–0.7050; Aegina 0.7041–0.7068 and Methana 0.7058–0.7067 though the lowest values observed in each centre of ca. 0.7040 is consistent with a mantle source (see review by Keller 1982).

Main Series basalts have comparable major and trace element compositions to those of high alumina calc-alkaline basalts erupted in many other orogenic provinces worldwide (cf. numerous analyses in Thorpe 1982) suggesting that the petrogenetic processes involved in generating high alumina basalts are not random and not restricted to specific tectonic and geographic settings. The chemical variation shown by the more evolved basaltic andesite, andesite, dacite and rhyodacite lavas of the Main Series is also comparable to that observed in other calc-alkaline basalt – andesite – rhyolite suites that are thought to have been generated by the crystal fractionation of a parental basalt magma (e.g. Rabaul and Talasea volcanoes, New Britain; Heming 1974; Arth 1981).

Discussion

The Quaternary – Recent volcanism of Santorini is intimately connected with subduction related processes as Mediterranean lithosphere sinks into the upper mantle beneath the Aegean region. The existence of a low Q region above the Benioff zone at a depth of some 120 km beneath the Aegean has been shown by Papazachos and Comninakis (1978), supporting the view that partial melting of the mantle asthenosphere wedge above the subducting plate may generate primitive basaltic liquids.

However, the relatively low Mg numbers (0.59–0.67) and low MgO, Cr and Ni contents of Main Series basalts preclude even the least fractionated basalt compositions from representing primitive liquids. Nicholls (1978) showed that Main Series basalts could represent primitive liquids which had subsequently undergone fractionation of ca. 6–12 wt.% olivine, 4 wt.% clinopyroxene and 0.5 wt.% Cr-spinel prior to eruption. The absence of a negative Eu anomaly in all least fractionated basalts (Fig. 7) supports the absence of plagioclase as a crystallising phase during this early crystal fractionation. Similarly, Osborn (1976) proposed that liquids analogous to the least fractionated Main Series basalts could be generated by partial melting of mantle peridotite at a minimum on the olivine – spinel – pyroxene boundary curve, as suggested by experimental studies of Mg_2SiO_4–Fe_3O_4–$CaAl_2Si_2O_8$–SiO_2 at a pressure of 10 kbar, followed by limited olivine, pyroxene and Cr-spinel separation on ascent. In the experimental system, this early stage of fractionation occurs at pressures > 8 kbar, the maximum at which anorthite and forsterite coexist in basaltic liquids in this system (Osborn 1976). For the Main Series magma, with plagioclase rather than anorthite present, the maximum pressure for olivine and plagioclase compatibility is about 20 kbar (cf. Osborn 1983), implying that this early fractionation occurred at pressures greater than 20 kbar within the Sub-Aegean mantle. This early high pressure fractionation may also help to generate the high SiO_2, Al_2O_3 and relatively high Fe contents of Main Series basalts as proposed by Osborn (1976).

The trace element concentrations of the primitive basalts parental to Main Series lavas has been estimated by adding 12 wt.% olivine, 4 wt.% clinopyroxene and 0.5 wt.% Cr-spinel to the least evolved basalt (M55) and by assuming appropriate mineral/liquid distribution coefficients from the literature. Primitive Main Series basalts may have the following estimated trace element concentrations – Sc 44 ppm; V 280 ppm; Cr 600 ppm; Co 56 ppm; Ni 240 ppm; P 300 ppm; Ti 4300 ppm; Rb 8 ppm; Sr 190 ppm; Y 16 ppm; Zr 45 ppm; Nb 2 ppm; La 5.5 ppm; Yb 1.7 ppm; Ba 90 ppm; Hf 2.0 ppm; Ta 0.18 ppm and Th 2.0 ppm.

This primitive composition is significantly LIL element enriched and shows marked depletions in all high charge/radius elements P, Ti, Zr, Nb and Ta on a chondrite normalised diagram (Fig. 9). The LIL enrichment and relatively high Sr^{87}/Sr^{86} ratios (0.7047–0.7051) of Main Series basalts, and of calc-alkaline magmas in general, cannot be

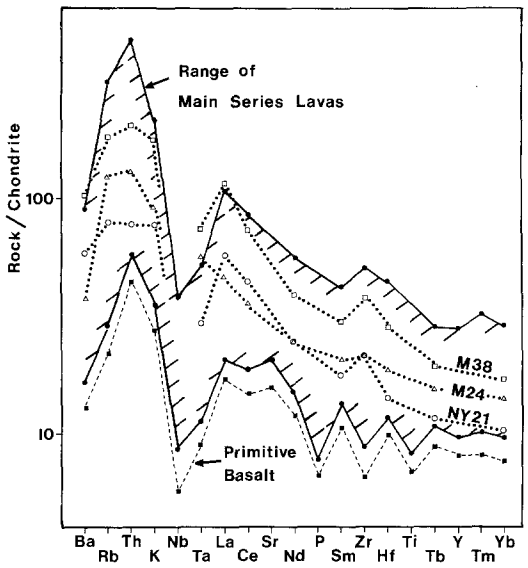

Fig. 9. Chondrite normalised patterns for the range of Main Series lavas and their estimated primitive basalt composition compared with patterns for lavas from other Hellenic Arc volcanic centres. NY 21 – basaltic andesite from Nisyros; M24 – andesite from Milos; M38 – dacite from Nisyros (Innocenti et al. 1981). Sr, Ti and P concentrations ignored in all evolved compositions due to plagioclase, magnetite and apatite crystallisation which distorts patterns. Normalising factors all chondritic (except Rb, K and P which are primitive mantle values) from Thompson et al. (1982)

accounted for by partial melting of unmodified mantle peridotite and are generally attributed to models involving melting of upper mantle itself enriched by interaction with LIL and isotopically enriched fluids released by partial melting or dehydration of the subducting lithospheric slab (e.g. Nicholls 1978). Explanations for the marked depletions in the high charge/radius element contents of Main Series and other orogenic magmas are unclear though they may reflect the presence of accessory minerals such as rutile, ilmenite, sphene, zircon and apatite as residual phases during partial melting under f_{O_2} and P_{H_2O} enriched conditions (Saunders et al. 1980).

All subsequent crystal fractionation involved calcic plagioclase + olivine with clinopyroxene implying pressures up to 20 kbar (Osborn 1983). Constraints on the physical conditions during crystallisation of the Main Series are poor and await more detailed mineralogical studies. However, experimental studies on basalts M84, M86 and basaltic andesite M85 have indicated liquidus temperatures of ca. 1,200–1,160° C and water contents of ca. 2 wt.% at pressures of 10–15 kbar for basic magmas of the Main Series (Osborn and Rawson 1980; Osborn and Boctor 1981). Osborn (1983) suggested a pressure of 14 kbar from a comparison of the TiO_2 contents of natural and experimental magnetites produced under the above conditions. From Fe–Ti oxides, Nicholls (1968, 1971) estimated temperature and oxygen fugacity levels of $T=1{,}150°$ C and $f_{O_2}=10^{-9}$ for basalt M54 (groundmass); $T=1{,}000°$ C and $f_{O_2}=10^{-11}$ for andesite M214 (phenocrysts); $T=950°$ C and $f_{O_2}=10^{-12}$ for andesite M212 (groundmass) and $T=890°$ C and $f_{O_2}=10^{-13}$ for rhyodacite M294, though more recent work indicates greater magmatic f_{O_2} levels above the NNO buffer (Osborn and Rawson 1980).

These pressure estimates suggest that the separation of calcic plagioclase + augite + olivine from liquids analogous to the observed least-fractionated Main Series basalts occurred at depths of ca. 30–50 km possibly in magma chambers close to the base of the crust beneath the Aegean. Further crystal fractionation may occur as these basaltic and more evolved liquids ascend through and lose heat to the lower sialic Aegean crust. Increasing viscosity and relatively high densities due to increasing iron contents prior to magnetite crystallisation may cause andesitic liquids to stagnate within the upper Aegean crust and to establish high level andesitic to rhyodacite magma chambers beneath Santorini, a view supported by the predominantly intermediate to silicic composition of the pyroclastic deposits erupted from the southern volcanic centres. Continued separation of plagioclase, augite, hypersthene, magnetite and apatite from andesitic liquids in these chambers may generate dacite and rhyodacite magmas as extreme residual liquids of the parental basalt (up to 84% crystallisation). The occurrence of caldera collapse during several eruptions of Santorini suggests that these andesitic and less dense and hence overlying dacite to rhyodacite chambers were at a relatively high crustal level and at possibly only a few kms depth beneath the volcano.

The establishment of high level andesitic to rhyodacite magma bodies beneath the southern volcanic centres of Santorini may have formed a shadow zone through which ascending basic magmas could not penetrate. Any high temperature basic magmas ascending into these larger, lower temperature magmas may cause mixing, convection and vesiculation and help to promote paroxysmal eruptions of the volcano in the manner outlined by Sparks et al. (1977). Hence, predominantly basaltic and basaltic andesite lavas and dyke rocks have been erupted from the northern centres which lie outside or are tectonically isolated from the higher level andesitic to rhyodacite chambers beneath the southern volcanic centres.

Similar volcanological considerations may also account for the predominance of basic lavas and silicic pyroclastics within the eruptive products of Santorini. Whereas less viscous basic magmas have been erupted from fissure systems in the north, the highly explosive eruptions of the southern volcanoes may have preferentially tapped less dense, overlying rhyodacite magma at the expense of less evolved, more dense, underlying andesitic magmas. Although Santorini has erupted large volumes of silicic magma, now represented in the thick pyroclastic deposits of the volcano and surrounding seafloor, volume considerations do not necessarily preclude crystal fractionation of a parental basalt magma as a viable mechanism in generating Main Series lavas. In absolute terms, volumes of 5–15 km^3 (dense rock equivalent) have been estimated for the rhyodacite magma erupted during the large Minoan eruption of Santorini (Pichler and Friedrich 1980; Sparks and Huang 1980). Depending on the exact density values chosen, such a volume of rhyodacite magma, representing some 16% by weight of a parent basalt magma, would require a volume for the parent basalt of some 25–75 km^3 at depth, a volume which is not considered prohibitive given recent estimates of magma volumes beneath other volcanoes (e.g. 1,600 km^3 beneath Etna; Sharp et al. 1980).

Appendix I

Analytical procedures: Analysis of Main Series lavas for P, Sc, Ti, V, Cr, Co, Ni, Rb, Sr, Y, Zr and Nb was carried

out in the Department of Earth Sciences, University of Cambridge by XRF using a Siemens SRS spectrometer. Routine peak to background analysis was carried out on pressed powder pellets and full dead time, interference, background and mass absorption corrections applied. Calibrations were constructed from a range of international rock standards. Sc, Cr, Co, REE, Ba, Hf, Ta and Th abundances were determined by instrumental neutron activation analysis (INAA) at the Scottish Universities Research and Reactor Centre, East Kilbride. Details of the analytical techniques and counting schedules employed have been given by Whitley et al.(1979). Percentage analytical errors (2σ) have been estimated from counting statistics as P (8%); Sc (2%); V (10%); Cr, Co, Ni (5%); Rb (6%); Sr (4%); Y (9%); Zr (4%); Nb (20%); La (1.5%); Ce (2.8%); Nd (5%); Sm (1.5%); Eu (2%); Gd (10%); Tb (4%); Tm (12%); Yb (2.5%); Lu (2%); Ba (7%); Ta (9%); Th (8%). Major element determinations of phenocryst phases in Main Series lavas were carried out by EDS microprobe in the Department of Earth Sciences, University of Cambridge using analytical techniques reported by Sweatman and Long (1969).

Acknowledgements. This work was carried out during tenure of a Natural Environment Research Council postgraduate studentship, receipt of which is gratefully acknowledged. The Department of Earth Sciences, University of Cambridge provided financial assistance towards the Neutron Activation analysis in this study. I should like to thank Dr. S.O. Agrell for releasing the specimens from the Department collection and N. Charnley and A.B. Moyes for their help with microprobe, computing and INAA work. Dr. P. Potts of the Open University kindly carried out REE analysis of 8 samples. Finally, I should like to thank E.F. Osborn, I.A. Nicholls, A.D. Saunders, J.A. Pearce, J. Huijsmans, T. Druitt, J. Wolff and N. Rogers for helpful comments on an earlier draft of this paper.

References

Allègre CJ, Treuil M, Minster JF, Minster B, Albarade F (1977) Systematic use of trace elements in igneous process, Part I. Fractional crystallisation processes in volcanic suites. Contrib Mineral Petrol 60:57–75

Arth JG (1981) Rare earth element geochemistry of the island arc volcanic rocks of Rabaul and Talasea, New Britain. Geol Soc Am Bull 92:858–863

Banks R (1979) The use of linear programming in the analysis of petrological mixing problems. Contrib Mineral Petrol 70:237–244

Comninakis PE, Papazachos BC (1980) Space and time distribution of the intermediate focal depth earthquakes in the Hellenic Arc. Tectonophys 70:T35–T47

Drake MJ, Weill DF (1975) Partition of Sr, Ba, Ca, Y, Eu^{2+}, Eu^{3+} and other REE between plagioclase feldspar and magmatic liquid: an experimental study. Geochim Cosmochim Acta 39:689–712

Durr St, Altherr R, Keller J, Okrusch M, Seidel E (1978) The Median Aegean Crystalline Belt: Stratigraphy, structure, metamorphism, magmatism. In: Alps, Apennines, Hellenides (Closs H, Roeder D, Schmidt K eds), pp 455–477. Stuttgart: Schweizerbart

Eggler DH, Osborn EF (1982) Experimental studies of the system $MgO-FeO-Fe_2O_3-NaAlSi_3O_8-CaAl_2Si_2O_8-SiO_2-$ a model for sub-alkaline magmas. Am J Sci 282:1012–1041

Evensen NM, Hamilton PJ, O'Nions RK (1978) Rare earth abundances in chondritic meteorites. Geochim Cosmochim Acta 42:1199–1212

Fytikas M, Guiliani O, Innocenti F, Marinelli G, Mazzuoli R (1976) Geochronological data on recent magmatism of Aegean Sea. Tectonophys 31:T29–T34

Gill JB (1978) Role of trace element partition coefficients in models of andesite genesis. Geochim Cosmochim Acta 42:709–724

Gill JB (1981) Orogenic andesites and plate tectonics. (Mineral and Rocks Vol 16), pp 390. Berlin-Heidelberg, Springer Verlag

Green TH, Watson EB (1982) Crystallization of apatite in natural magmas under high pressure, hydrous conditions, with particular reference to 'orogenic' rock series. Contrib Mineral Petrol 79:96–105

Hammer CU, Clausen HB, Dansgaard W (1980) Greenland ice sheet evidence of post-glacial volcanism and its climatic impact. Nature 288:230–235

Heming RF (1974) Geology and petrology of Rabaul caldera, Papua New Guinea. Geol Soc Am Bull 85:1253–1264

Hoefs J (1978) Oxygen isotope composition of volcanic rocks from Santorini and Christiani. In: Thera and the Aegean World. Vol I (Doumas C ed), pp 163–170. Athens: Tsiveriotis

Innocenti F, Manetti P, Peccerillo A, Poli G (1981) South Aegean volcanic arc: geochemical variations and geotectonic implications. Bull Volcanol 44:377–391

Irvine TN, Baragar WR (1971) A guide to the chemical classification of the common igneous rocks. Can J Earth Sci 8:523–548

Irving AJ (1978) A review of experimental studies of crystal/liquid trace element partitioning. Geochim Cosmochim Acta 42:743–770

Keller J (1982) Mediterranean island arcs. In: Andesites (Thorpe RS ed), pp 307–325. Chichester: Wiley

Luhr JF, Carmichael ISE (1980) The Colima volcanic complex, Mexico. Contrib Mineral Petrol 71:343–372

McKenzie D (1978) Active tectonics of the Alpine – Himalayan belt: the Aegean Sea and surrounding regions (tectonics of the Aegean region). Geophys JR Astr Soc 55:217–254

Miyashiro A (1974) Volcanic rock series in island arcs and active continental margins. Am J Sci 274:321–355

Nicholls IA (1968) Petrology and geochemistry of Santorini lavas. Unpubl PhD thesis, Univ of Cambridge, pp 275

Nicholls IA (1971) Petrology of Santorini volcano, Cyclades, Greece. J Petrol 12:67–119

Nicholls IA (1978) Primary basaltic magmas for the pre-caldera volcanic rocks of Santorini. In: Thera and the Aegean World. Vol I. (Doumas C ed), pp 109–120. Athens: Tsiveriotis

Nicholls IA, Harris KL (1980) Experimental rare earth element partition coefficients for garnet, clinopyroxene and amphibole co-existing with andesitic and basaltic liquids. Geochim Cosmochim Acta 44:287–308

O'Hara MJ, Mathews RE (1981) Geochemical evolution in an advancing, periodically replenished, periodically tapped, continuously fractionated magma chamber. J Geol Lond 138:237–277

Osborn EF (1976) Origin of calc-alkali magma series of Santorini volcano type in the light of recent experimental phase equilibria studies. In: Proc Int Cong Therm Waters, Geotherm Energy, Volcanism Med Area, Vol 3, pp 154–167, Athens

Osborn EF (1979) The reaction principle. In: The evolution of the igneous rocks – fiftieth anniversary perspectives (Yoder HS Jnr ed), pp 133–170, Princeton: Univ Press

Osborn EF (1983 in press) On the significance of the spinel phase in subalkaline volcanic magmas. Mem Geol Soc China 5 (Taipei)

Osborn EF, Boctor NZ (1981) Some additional observations on magnetite in calc-alkaline volcanic rocks. Carnegie Inst Wash Yearb 80:324–327

Osborn EF, Rawson SA (1980) Experimental studies of magnetite in calc-alkaline rocks. Carnegie Inst Wash Yearb 79:281–285

Papazachos BC, Comninakis PE (1978) Geotectonic significance of the deep seismic zones in the Aegean area. In: Thera and the Aegean World. Vol I. (Doumas C ed), pp 121–129. Athens: Tsiveriotis

Pe GG, Gledhill A (1975) Strontium isotope ratios in volcanic rocks from the southeastern part of the Hellenic Arc. Lithos 8:209–214

Peacock MA (1931) Classification of igneous rock series. J Geol 39:54–67

Pearce JA, Norry MJ (1979) Petrogenetic implications of Ti, Zr, Y and Nb variations in volcanic rocks. Contrib Mineral Petrol 69:33–47

Pichler H, Friedrich WL (1980) Mechanism of the Minoan eruption of Santorini. In: Thera and the Aegean World. Vol 2 (Doumas C ed), pp 15–30

Pichler H, Kussmaul S (1972) The calc-alkaline volcanic rocks of the Santorini group (Aegean Sea, Greece). N Jb Mineral Abh 116:268–307

Pichler H, Kussmaul S (1980) Comments on the geological map of the Santorini Islands. In: Thera and the Aegean World. Vol 2. (Doumas C ed), pp 413–427. Athens: Tsiveriotis

Puchelt H (1978a) Geochemical implications for the Santorini Island group (Aegean Sea, Greece). In: Alps, Apennines, Hellenides (Closs H, Roeder D, Schmidt K eds), pp 489–493, Stuttgart, Schweizerbart

Puchelt H (1978b) Evolution of the volcanic rocks of Santorini. In: Thera and the Aegean world. Vol 1 (Doumas C ed), pp 131–146. Athens, Tsiveriotis

Puchelt H, Hoefs J (1971) Preliminary geochemical and strontium isotope investigations on Santorini rocks. In: Ist International Scientific Congress on the volcano of Thera. pp 318–327. Athens

Saunders AD, Tarney J, Weaver SD (1980) Transverse geochemical variation across the Antarctic peninsula: implications for the genesis of calc-alkaline magmas. Earth Planet Sci Lett 46:344–360

Sharp ADL, Davis PM, Gray F (1980) A low velocity zone beneath Mount Etna and magma storage. Nature 287:587–591

Sparks RSJ, Huang TC (1980) The volcanological significance of deep-sea ash layers associated with ignimbrites. Geol Mag 117:425–436

Sparks RSJ, Sigurdsson H, Wilson L (1977) Magma mixing: a mechanism for triggering acid explosive eruptions. Nature 267:315–318

Sweatman TR, Long JVP (1969) Quantitative electron probe microanalysis of rock forming minerals. J Petrol 10:332–379

Thompson RN, Dickin AP, Gibson IL, Morrison MA (1982) Elemental fingerprints of isotopic contamination of Hebridean Palaeocene mantle-derived magmas by archean sial. Contrib Mineral Petrol 79:159–168

Thorpe RS (1982) Andesites. (Orogenic andesites and related rocks). 724 pp, Chichester, Wiley

Treuil M, Varet J (1973) Critères volcanologiques, petrologiques et géochimiques de la genèse et de la differenciation des magmas basaltiques: exemple de l'Afar. Bull Soc Geol France, 7eme Serie, 15:401–644

Villemant B, Jaffrezic H, Joron J-L, Treuil M (1981) Distribution coefficients of major and trace elements; fractional crystallization in the alkali basalt series of Chaîne des Puys (Massif Central, France). Geochim Cosmochim Acta 45:1997–2016

Whitley JE, Moyes AB, Bowden P (1979) Determination of rare earth elements in geological samples by neutron activation analyses. J Radioanal Chem 48:147–158

Wright TL,Doherty PC (1970) A linear programming and least squares computer method for solving petrological mixing problems. Geol Soc Am Bull 81:1995–2008

Received January 19, 1983; Accepted June 16, 1983